EASY TO IMPLEMENT DIAGNOSTICS

OF A GLOW DIELECTRIC BARRIER DISCHARGE

F. Massines and P. Ségur*
Laboratoire de Génie Electrique, * Centre de Physique des Plasmas et de leurs Applications
Université Paul Sabatier, 118 route de Toulouse, 31062 Toulouse Cedex, France. massines@lget.ups-tlse.fr

1 Introduction

It is relatively easier to generate plasma at atmospheric pressure rather than low pressure. In retaliation, due to the short mean free path of different particles, the diagnostics giving microscopic characteristics are more difficult to implement. This, for example, is the case of Langmuir probe or mass spectrometry although solutions have been put forward [1]-[3]. Likewise, the strong contribution of the excited state quenching can render optical characterization result interpretation difficult. Nevertheless, there are easy to implement basic diagnostics like optical emission spectroscopy, the ultra rapid photography or the discharge current measurement. A possible approach to get to the microscopic data consists in associating the experimental results with the results of a numerical model. This is the approach undertaken for the study of a glow dielectric barrier discharge (DBD) and is described in the following text in order to illustrate the possibilities of those easy to implement diagnostics supported by the analysis of surfaces having interacted with the plasma.
DBD are low temperature pulsed discharges usually working at atmospheric pressure [4]-[5]. They are typically obtained between two coplanar electrodes separated by a gap of some millimetres and excited by a low frequency voltage. At least one of the electrodes is covered by a dielectric. These discharges are transient ones. Then, time resolved diagnostics are always powerful to study the discharge development and to follow the energy transfer in the afterglow. The diagnostic set-up characteristics depend on the type of DBD. Streamers have a duration of some tenths of nanoseconds and a radius of about 100µm. They develop more or less randomly. Then, their characterization is not easy to realize despite a lot of methods being used over a century [6-12]. Glow DBD have only been studied for fifteen years. Due to their dielectric barrier they are also transient discharges but their duration is in the range of microseconds, each discharge covers the entire surface of the electrodes and the breakdown voltage is a constant [13]. Characterization difficulties come more from the limited experimental conditions leading to such a discharge [Kogoma et nous] and the small gas gap value. As glow DBD is easily destabilized, only non-invasive diagnostics can be used like optical diagnostics and discharge current measurements but not Langmuir probe. Of course, numerical modelling is of great help as well as the analysis of a surface, which has interacted with the discharge. In the following text the interest of discharge current measurements, numerical modelling, time resolved emission spectroscopy and ultra-short photography as well as surface transformations will be illustrated.

1 Electrical characterization

At atmospheric pressure, the most common electrical diagnostic of low frequency discharges consists in the measurement, as a function of time, of the voltage applied to the electrodes and the discharge current. A high frequency oscilloscope through a 50Ω resistor connected between one of the electrodes and the ground usually records the current. Some authors [14-15] replace the resistor through a capacitor to have Lissajous figures that is the discharge current integral, i.e., the charge as a function of the voltage.
Figure 1 shows 3 examples of discharge current and applied voltage oscillograms measured by the experimental set-up presented in figure 2. It is constituted of two plane parallel electrodes separated by a gas gap of 5mm for helium experiments and 1mm for nitrogen one. A 0.6 mm thick alumina plate covers each electrode. The discharge set-up is inside a vessel allowing a control of the discharge atmosphere in the ppm range. The oscilloscope is a TDS 784A Tektronix.
The figure1a is a typical oscillogram of a filamentary discharge. Each current pulse corresponds to at least one streamer. As the radius of electrodes is about 200 times that of a streamer, several streamers can independently develop at the same time. The discharge current is the sum of the streamers current, thus streamers developing simultaneously cannot be distinguished. Such a measurement is not trivial because the current increases in some nanoseconds, which corresponds to gigahertz in frequency. The impedance of the detection circuit has to be carefully controlled. To avoid these problems, some authors measured the total light emitted by the discharge using a high speed photo-multiplier [16]. The transient nature of a DBD can be easily understood [5] looking at the equivalent electrical circuit (Fig. 3). C_{ds} is a capacitance whose plates are the electrodes and the section of the discharge in contact with the solid dielectric and the insulating part is the dielectric barrier (2x0.6mm of alumina). As soon as the breakdown occurs, Cds is charged by the discharge current. The voltage applied to this

capacitance increases according to equation 1. The applied voltage being constant during the considered time period (20ns) the voltage applied to the gas decreases (Eq. 2) and the discharge is stopped. This is why DBDs are of great interest in applications as they efficiently avoid the transition to arc, which is easy to observed at atmospheric pressure.

$$V_{ds}(t) = 1/C_{ds}\int_{to}^{to+t} I(t).dt + V_{ds}(t_0) \quad (1)$$

$$V_A(t) = V_g(t) + V_{ds}(t) \quad (2)$$

Figures 1b and 1c compare the discharge current of a glow DBD in He and in N_2. In the two cases, the current is composed of only one peak per half cycle and the duration of this peak is very large compared to that of a streamer (Fig.1a): 3 µs and 200µs respectively in He and in N_2. Looking further into details, significant differences are observed according to the atmosphere. The current peak is sharper in He. Typically, its amplitude is 10 times higher and its duration 10 times lower.

In case of a glow DBD, the section of the discharge is known (it is equal to the electrode surface) and the discharge uniformly charges the surface of the entire dielectrics covering the electrodes. The voltage applied to the gas can then be calculated rather accurately: C_{ds} (Fig. 2b) and then V_{ds} and V_g are calculated following equation 1 to 3 assuming $V_{ds}(t_0)$ to be such that $\int_0^T V_g dt = 0$, T being the cycle duration.

$$Cds = \varepsilon_o \varepsilon_r S/d \quad (3)$$

where ε_o is the void permittivity, ε_r is the dielectric relative permittivity, S is the discharge section, d is the dielectric thickness

In He (Fig. 1d) , for a gas gap of 5 mm, it decreases from 1.4 kV at the instant of the breakdown to more or less 0V during the discharge current peak. This behaviour clearly illustrates the role of the dielectric as is usually: the discharge is stopped due to the decrease of the voltage applied to the gas induced by the charge of capacitance C_{ds}.

In N_2 (Fig. 1b), V_g continues to increase after the breakdown and then saturate around 5 kV for a 1 mm gap. The gas voltage is higher at the maximum current than at the beginning of breakdown. This is explained by the fact that the increase of the current and thereby the charge of C_{ds} (Eq. 1) is too slow as compared to the variation of the applied voltage in order to induce a significant decrease of the gas voltage (Eq.2). Then the current is not limited by the decrease in the applied voltage to the gas. Actually, it is limited because the impedance of the gas becomes lower than that of the dielectric barrier. In an electrical circuit the higher impedance in series dictates the limits of the current. Equation 4 gives the expression for the C_{ds} and the gas impedances.

Between two discharges, the gas can be considered as a pure insulating medium. Its equivalent capacitance is 30 pF for a volume of 34 mm^3 (85x40x1 mm^3). The system is purely capacitive and is composed of the dielectric capacitance, C_{ds}, (220pF) in series with the gas capacitance, C_g. As shown in figure 4, the value of the lower capacitance, C_g, controls the behavior of the current whose variations are equal to $C_g dV_g/dt \approx C_g dV_A/dt$.

$$Z_{ds} = 1/C_{ds}\,\omega \qquad Z_g = 1/(C_g\,\omega + 1/Rg) \quad (4)$$

where Z is the impedance and ω the pulsation.

When breakdown occurs, electrons and ions are created in the gas, leading to a change in the impedance associated with the gas. It becomes lower than that of C_{ds}. The current passing through the discharge is then limited by the value of $C_{ds}dV_{ds}/dt$ ($\approx C_{ds}dV_A/dt$ as V_g is almost constant near the maximum of the current). For the sake of comparison, $C_{ds}dV_A/dt$, C_gdV_A/dt and the discharge current are presented in figure 4. The variations of the discharge current follows that of C_gdV_A/dt between two discharges and that of $C_{ds}dV_A/dt$ from around 50 µs after the breakdown to the end of the current peak.

Between the two previous situations, a transition phase exists during which the impedance of the discharge decreases from $Z_g=1/C_gw$ to a value lower than $Z_{ds}=1/C_{ds}w$. When the current is equal to $I_d=C_{ds}dV_A/dt$, no more current can pass through the dielectrics. The increase in the gas ionization is stopped. At this moment, the dielectrics control the discharge. V_A still increases while V_g is constant (or decreases slowly), so the variations of V_A are mainly applied to the dielectrics.

In conclusion, these results show how the current measurement allows to distinguish clearly between pure filamentary and glow DBD and how it points out to differences in the electrical behaviour of the glow DBD in the two gases considered.

The discharge current in between 2 discharges can also give information on the discharge behaviour. In between two filamentary DBD in series, no current is measurable while in between 2 glow DBD the current is never equal to zero, which shows that there is always a non negligible charges density in the gas gap. As shown in figure 1d, this is especially true when the polarity of the gas voltage is reversed. Memory effects at the origin of this behaviour have been clearly shown by the numerical modelling results.

3 Numerical modelling

Numerical modelling of dielectric barrier discharges has been undertaken since a long time for silent discharges [17],[18], essentially used for ozone production and for plasma display panel. In both cases, the numerical approach was based on the use of macroscopic equations (continuity, momentum transfer, energy conservation equations) and the treatment was made either in one or two dimensions in space. In these studies, direct

ionisation and Penning ionisation were usually assumed to be the main mechanisms responsible for the creation of new electrons. Usually, no complicated reactions between the ionic species of the discharge were taken into account.

Howether, to low pressures, in which direct ionization of molecules by electrons is the most important mechanism, atmospheric pressure discharges have very specific properties due to the fact that new reactions between heavy species are included. For example, in helium, reactions involving He_2^+ ions created through three body collisions are very important unlike at low pressures where only H_e^+ ions appear. It follows that in order to establish a realistic numerical model of a high-pressure discharge, the nature of the fundamental processes inside this discharge must be clearly identified as they may be very different from those occurring at low pressure.

Furthermore, the glow DBD is periodic and as the duration of the period is of the order of some microseconds, neutral heavy species do not move significantly during that period and thus are likely play an important role on the behavior of the discharge. It is then necessary to determine the concentration over space and time of the various neutral species created inside the gas gap. It follows that in this type of discharge, the equations that characterize the interactions between heavy neutral particles must be solved in exactly the same way as the equations involving charged particles.

The behavior of neutral and charged particles is determined by solving the continuity and momentum transfer equations together with the Poisson equation. As the discharge is homogeneous, its radial extension is longer than its length and a one-dimensional approach is sufficient. It is necessary to take into account all the collision processes involved in the production or destruction of electrons or ions. The mobility and diffusion coefficients for electrons and ions, the metastable diffusion coefficients as well as various reactions considered with the corresponding reaction rates have been given in a previous paper for He [13] and N_2 [19]. Photo-ionization mechanisms in the gas were not considered and ionic current only produced the secondary emission of electrons at the cathode. For all ions considered, the secondary emission coefficient was assumed to be constant and equal to 0.01

Comparison of the experimental and calculated discharge current and gas voltage permits to verify the model validity. The figure 5 shows the space distribution of the electrical field and the ion and electron densities when the discharge current is maximum in N_2 and in He. In He, the calculated features are clearly those of a low pressure glow discharge with a cathode fall of 400µm and a 3mm positive column for a 5mm gap. Ion and electron maximum density is some $10^{11}/cm^3$. In N_2, a different behavior is noticed. The shape of the electric field resembles that of a Townsend discharge with a pure cathode fall and no negative glow. The maximum electron density ($10^8/cm^3$) occurs at the anode and is lower than the ion density ($10^{11}/cm^3$). Taking into account the small variation of the electric field in the cathode fall we can note that the maximum rate of production of excited or ionized species by electron impact will be close to the anode while in He, it is near the cathode. To summarize, in both the atmospheres, the glow DBD is a glow discharge in the sense that secondary electrons are always due to ion bombardment of the cathode and the positive space charge maximum is always at the cathode, it is larger in case of He than in case of N_2. Then, in agreement with the discharge current measurements, the numerical modeling shows that glow DBD in N_2 is closer to a Townsend discharge than in He. In the two cases the DBD is a sub-normal glow discharge.

Numerical modeling also permits determination of the dominant energy transfer mechanisms. For example, in N_2, the main ionization mechanism is not due to direct electron-molecule ionization, but due to indirect ionization through the collision between two metastable states of nitrogen (Eq. 5) (Figure 6). This mechanism depends on the metastable states density and not on the electrical field. As the life time of these states is long compared to the half-cycle excitation duration, electrons and ions are always created, even in between two discharge current peaks. This is why the current is never equal to 0 in between two glow DBDs.

$$\begin{aligned} &N_2(a'^1\Sigma_u^-) + N_2(A^3\Sigma_u^+) \rightarrow N_4^+ + e \\ &N_2(a'^1\Sigma_u^-) + N_2(a'^1\Sigma_u^-) \rightarrow N_4^+ + e \end{aligned} \qquad (5)$$

The numerical model shows that in He, ionisation is stopped in between two discharges because at atmospheric pressure, the $He2^3s$, which is the main He metastable state, is efficiently transformed in the dimmer He_2 by collision with two He atoms at the fundamental level. As the consequence, the lifetime of He metastable state at atmospheric pressure is of 8 µs that is low compared to the time between two discharges. Then, in that case, the discharge current observed when the gas voltage is close to zero is due to electrons trapped in the positive column.

The numerical modeling allows the interpretation of the discharge current, not only in terms of the order of magnitude of the space and time densities of the electrical field and the charged and excited particles but also in terms of the main mechanisms controlling the discharge.

4 Time resolved UV visible optical emission spectroscopy

Optical emission spectroscopy (OES) gives information from the discharge radiative excited states. Rotational and vibrational spectra can be studied to deduce temperature [20]. Electron density can be deduced from line Stark broadening [6]. This method is commonly used because it is non-invasive and easy to implement. The pressure increase does not change the experimental conditions. Of course, when studying a transient discharge it is interesting to have a time resolved detection like an intensified CCD camera to identify fast and slow excitation mechanisms. Usually the set-up includes a collimated optical fibber or a lens to guide the plasma light to the entrance slit of a monochromator that separates the light according to the wavelength and a detection system such as a photo-multiplier or a CCD camera. To achieve time resolved measurements, the detector system has to be synchronized with the discharge. This is easy to realise when the discharge is periodic like in the case of glow DBD but not in the case of filamentary DBD. Not only the time resolution has to be of the order of nanoseconds but also the voltage under which the streamer develops is not constant. Thus the synchronisation of the discharge with the detection is not easy to realise. Nevertheless, there are solutions such as the cross-correlation method [21].

In our case, DBD plasma light has been analysed by means of a SPEX 270 M (focal length 27 cm) spectrometer with 3 gratings (150, 1200 and 2400 gr.mm^{-1}) coupled to an intensified CCD camera detector with a time resolution of 10^{-8} s. The plasma light was focused at the entrance slit of the spectrometer. The detection was synchronized with the applied voltage that has the same periodicity as the current. Of course, with this system, it is not possible to study a streamer development but spectra in between two series of filamentary DBD can be recorded to enable the determination of long life time species. In case of glow DBD, as the discharge establishes itself slowly and is periodic, the discharge development can be carefully studied. This has been done in He and N_2. Figure 7 illustrates the results obtained in He. According to equation 6, the N_2^+ emission can be considered having a signature of the first He metastable state, (N_2^+(B) is the excited state at the origin of the first negative system which is observed). This emission is more or less proportional to the discharge current, which confirms that the He2^{3}s lifetime is short compared to the discharge time. Only OH emission is observed in the after glow. This emission has been attributed to H_2O^+ ion recombination, these ions being created by collision with He_2.

$$He(2^3S) + He + N_2 \rightarrow 2\,He + N_2^+(B) \quad (6)$$

According to figure 8, very different spectra can be obtained in N_2 at atmospheric pressure with the same electrode configuration at excitation of 1 and 4 kHz. This small frequency variation permits a changeover from glow to filamentary DBD. A clear difference emerges between these spectra corresponding to the two kinds of discharge: whereas NOγ system, N_2 2nd positive system and the green transition ($O(^1S)N_2$* --> $O(^1D)N_2$ at 557.7 nm) represent the most intense emission bands in and out of the discharge for the glow DBD, only N_2 (2nd+) and CN bands appear distinctly for the filamentary DBD. These differences are particularly noticeable outside the discharge.

The impurities (O and C) come essentially from the surface etched by the discharge showing that OES can be very sensitive to impurities and, unfortunately, not at all to high density particles. The excitation mechanisms are given below. When the discharge is switched on, the excitations are mainly due to electronic collisions (Eq. 7-9). When the discharge is switched off, the contribution of electrons decreases drastically because of the low value of the electrical field and the emissions are due to radical recombination (Eq. 11) in the filamentary DBD and due to collision with metastable states (Eq 9 and 13) in the glow DBD. Then, differences observed between filamentary and glow DBD can be is explained by the difference in N_2 metastable state density.

N_2 2nd positive system:

$$N_2 + e \rightarrow N_2^* + e \quad (7)$$

NOγ system:

$$NO + e \rightarrow NO^* + e \quad (8)$$

$$NO + N_2(A^3\Sigma_u^+) \rightarrow NO^* + N_2 \quad (9)$$

CN violet system:

$$CN + e \rightarrow CN^* + e \quad (10)$$

$$CN + N_2(v) \rightarrow CN^* + N_2 \quad (11)$$

$$C + N \rightarrow CN^* + N_2 \quad (12)$$

ON_2 band:

$$O + N_2(A^3\Sigma_u^+) + N_2 \rightarrow ON_2^* + N_2 \quad (13)$$

These examples illustrate the way OES gives indirect information on long lifetime species of the discharge, which play a major role in glow DBD.

4 Short exposure time photographs

Photographs are taken with an intensified CCD camera triggered by the voltage applied to the gas gap or via an optical fiber detecting the discharge onset. When the discharge current is periodic, a delay allows the follow up

of the evolution of the light distribution in the gas gap as a function of the current. Pictures can also be taken through the electrode using glass plate covered by ITO [5]. By adjusting the delay, short exposure time photographs of the discharge cannshow how and where the discharge develops. This method can be very useful to distinguish between discharges, which have the same electrical behavior but not the same space evolution.
Gas gap photographs taken during the initiation of He glow DBD with a 100 ns exposure time are presented in figure 9a. The development of the light intensity with time does not show a radial localization of the discharge. The luminous area near the anode observed since the first picture is the memory of the previous discharge. Its intensity decreases with time even when the new discharge is turned on. The light first occurs everywhere in the gap (Photo. 1) and then its intensity increases in the gap half adjacent to the cathode. This behavior agrees well with Townsend breakdown mechanism (16, 21) which presumes successive generation of avalanches and a discharge self sustained by cathode secondary emission due to photon ionization of the electrode, there after due to ion bombardment since ions have enough time to move to the cathode before space charge induces field localization. Then, since ions are less mobile than electrons, a positive space charge occurs producing a more important variation of the field near the cathode and the formation of a cathode fall leading to a glow discharge. The numerical modeling has validated this interpretation. At the maximum of the current, pictures were taken with an exposure time of 10 ns (Fig. 10b), i.e., the order of magnitude of the lifetime of a streamer. No channel appears and 3 luminous domains can be distinguished: there is an area of high light intensity near the cathode followed by a dark space of about the same thickness (about 1 mm) and then a rather luminous zone of 3 mm. This is exactly the feature of a glow discharge with the cathode and the negative glow (that can not be distinguished at a high pressure), the Faraday dark space and the positive column.
In He, a decrease of the excitation frequency from 8 to 3 kHz induces the transition from glow to filamentary DBD. This transition is continuous, the first step cannot easily be deduced from discharge current measurements but they are clearly shown by short exposure time pictures taken during the breakdown (Fig. 9b). The light first occurs near the anode and then it increases a lot before crossing the gap. The cathode is first reached on one side of the electrode. After that the pictures are very similar to those taken in a glow DBD. The structures of the negative and the cathode glow, the Faraday dark space and the positive column (Fig. 9b) are also observed at the maximum of the current and thereafter. In the case presented, the radius of the discharge seems to be equal to that of the electrode but the radial uniformity is not as good as it is in the case of glow DBD. For an excitation frequency of 4 kHz, the same behaviour is observed but the first luminous zone has a radius of about 0.5 cm. Thus the transition discharge has an intermediate behaviour between that of a filamentary DBD and a glow DBD. The mode of propagation from the anode to the cathode is similar to that of a streamer but the channel radius is at least 500 times larger than that of a streamer and the development time 150 times longer. Such a behaviour is attributed to the coupling of several streamer avalanches. Differences with glow DBD are only observed at the beginning of the discharge. The fact that the discharge does not cover the entire electrode surface uniformly at its beginning also explains the non-periodicity of the current which is observed as well.
Short exposure time photographs allow to conclude that in He, by varying the frequency from 1 to 20 kHz, 3 kinds of discharges can be obtained: filamentary DBD from 1 to 2 kHz, glow DBD from 7 to 20 kHz and some thing in between the two which covers roughly the entire electrode surface and thus can be called homogeneous DBD.
The light distribution in the gap at the maximum discharge current illustrates the differences between He and N_2 glow DBD (figure 9b and 9c). These ten nanoseconds exposure time photographs show that in the two cases there is only one discharge channel covering uniformly the entire electrodes surface. But, if in He the low-pressure glow discharge structure is clearly observed, this is not the case in N_2 as the light is mainly on the anode side. In N_2, such a light distribution is observed from the beginning of the discharge to the current maximum. This appearance has been attributed to a Townsend discharge without the formation of a positive space charge large enough to induce the formation a positive column. These observations confirm the validity of the numerical modelling and the explanation of the discharge current behaviour in between the two discharges.

5 Surface analyses

The plasma active species interact with a surface and so the surface transformation depends on the physics and the chemistry occurring in the gas phase. Consequently, the study of the surface properties gives information on the discharge characteristics. This is illustrated by the evolution of a plastic (polypropylene) surface energy treated in a He DBD as a function of the discharge excitation frequency, all other parameters being maintained constant. The figure 11 represents the evolution of the contact angle of water drops deposited on the polypropylene treated surface as a function of the discharge excitation frequency. Smaller is the contact angle higher is the wettability and the level of surface transformation. Three different behaviour patterns can be distinguished. When increasing the DBD excitation frequency from 1 to 2 kHz the value of the angle is about 57°±5°, then from 4 to 7 kHz its value decreases to 32°±2° and from thereon it becomes frequency independent. The limiting frequencies of the different discharge regimes have been reported in the same figure. They have been determined from the discharge current measurements performed during the surface treatment and the short exposure time photographs. A clear correlation between the surface treatment and the discharge regime is

revealed. Surface chemical composition determined by Xray photoelectron spectroscopy (XPS), explains the higher wettability obtained with a glow DBD by a higher level of nitrogen incorporated in the surface. This can be reasoned from the physics of the discharge. The energy dissipated in the gas is nearly independent of the frequency but the spatial distribution depends on the discharge regime (Figure 9 and 10). Glow DBD is controlled by a cathode sheath which means that the main part of the electrical energy is dissipated in a layer, of about 500 μm thickness, near the cathode. This means that excitation and ionisation of the gas preferentially occurs in this area and so the majority of the ions and excited species (He metastables, He2) reach the cathode, which is the electrode where the sample is for half the time. In the case of filamentary DBD, the energy is more or less uniformly dissipated over the entire discharge channel bridging the anode with the cathode (5 mm). Then a lot of excited species and ions return to the fundamental level before reaching the electrodes and thereby encountering the film.

Moreover, since the main difference between filamentary and glow DBD treatment is the density of N at the surface, N_2^+ ions certainly play a dominating role. It is known that when an N_2^+ ion reaches the polymer it can recombine with an electron of the material, and if this recombination is a dissociative one ($N_2^+ + e \rightarrow 2\ N$) it releases an energy of some eV which is enough to break a chemical bound of the polymer. Then at the same time and at the same place, radicals are created on the polymer and in the gas, increasing considerably the probability of a reaction. This is confirmed by the emission spectra of filamentary and glow DBD (Fig. 12), which show that the N_2^+/N_2 ratio is higher in the case of the glow discharge. Then in case of He DBD, the simplest way to distinguish glow and streamer coupling discharge is not to take short exposure time pictures but to measure the water contact angle on a polypropylene film…

5 Conclusion

Results obtained in the case of glow DBD illustrate the interest of easy to implement diagnostics like discharge current measurements, optical emission spectroscopy, short exposure time photographs or even analysis of a surface after its interaction with the plasma. All these methods are useful because they are non invasive methods which can be implemented regardless of the type of discharge. Of course as these gas diagnostics allow time resolution, they are more powerful in case of transient discharges where it is interesting to separate rapid energy transfer due to electrons from slow ones due to charges recombination, radicals transformations, excitations by collision with metastables. Space resolution given by the optical methods, even by OES, is valuable because at a high pressure, the discharge constriction is often an important question mainly in a low temperature plasma, when the local power density has to be maintained under a certain level in order to avoid a too large temperature increase. The main limitation of these diagnostics is the fact that they do not easily lead to microscopic data and absolute values. Then, different observations in conjunction only allow determination of the main mechanisms. Of course, there are non-invasive diagnostics making available microscopic data that can be utilized at the atmospheric pressure. They are mainly optical methods. For example, V-UV absorption, Infra Red absorption, Laser Induced Fluorescence (LIF) which provide absolute values of particle density. Such diagnostics are very powerful and first attempts at atmospheric pressure are being carried out with the two last methods. As shown in this paper, another way to attain the microscopic level from macroscopic measurements consists in developing a numerical modeling closely related to the experimental observations.

6 Reference

[1] Belinov M.S., J. Phys. D :Applied Physics, Vol.33 (2000), 1683-1696.
[2] Alexeff I., Garland C., Weng-lock-Kang, Laroussi M., IEEE Int. Conf. On Plasma Science, Picataway, USA, 2000, 109.
[3] Kull A.E., Cappelli M. A., 27th IEEE Int. Conf. On Plasma Science, Picataway, USA, 2000, 120.
[4] Kogelschatz U., HAKONE VII, Greifswald, Allemagne, 10-13 Septembre 2000, 1-6.
[5] Eliasson B., Kogelschatz U., IEEE Trans. Plasma Sci.19 (1991) 309-322.
[6] Barmann P., Kroll S., Sunesson A., J. Phys. D :Applied Physics, Vol.29 (1996), 1188-1196.
[7] Sakai T,Shirasaka Y,Takada T,Yumoto M,7th Int. Conf. Gas Dis. and Appl.,Peter Peregunus,Stevenage,UK,1982,495-498
[8] Pfeiffer W, Fischer H, Applied Optics, Vol 20, N°14, (1981) 2328-2329.
[9] Tajalli H., Lamb D.W., Woolsey G.A., J. Phys. D :Applied Physics, Vol.22, (1989), 1497-1503.
[10] Zhu Y., Takada T., Sakais K. Demin Tu, Petrov N.I., J. Phys. D :Applied Physics, Vol.29, n°11,(1996), 2892-2900.
[11] Creyghton Y,Van Veldhuizen E.M.,Rutgers W.R.,IEE Proc. Science Measurements and Techno.,141, 2,(1994), 141-147.
[12] Petroc N.I., Avanskii V.R., Bombenkova N.V., Technical Physics, Vol. 39, (1994), 546-551.
[13] Massines F., Rabehi A., Decomps Ph., Ben Gadri R., Ségur P. and Mayoux Ch., Journal of Applied Physic, Vol.38, N°6, (1998), 2950-2957.
[14] Falkenstein Z., J.J. Coogan, J. Phys. D:Appl. Phys., 30(1997) 817-825
[15] Okazaki S., Kogoma M., Uehara M. and Kimura Y., J. Phys. D:Appl. Phys., 26(1993) 889-892
[16] Monette E,Bartnikas R.,Czeremuszkin G.,Latreche M.,Wertheimer M.E., 14th ISPC, Prague, 2-6 August 1999, 991-996.
[17] Creyghton YLM, Van Veldhuizen E.M., Rutgers W.R., IEE Proc. Sci. Meas. and Techno., 141, 2, (1994), 141-147.
[18] Petroc N.I., Avanskii V.R., Bombenkova N.V., Technical Physics, Vol. 39, (1994), 546-551.
[19] Ségur P. and Massines F., GD 2000, Glasgow, UK, Sept 2000, IL3
[20] Chelouah-A; Marode-E; Hartmann-G; Achat-S, J. Phys. D:Appl. Phys.,27 (1994),940-945.
[21] Brandebourg R., Kozlov K.V., Michel P., Wagner H.E., HAKONE VII, Greifswald, 10-13 Sept 2000, 189-193.

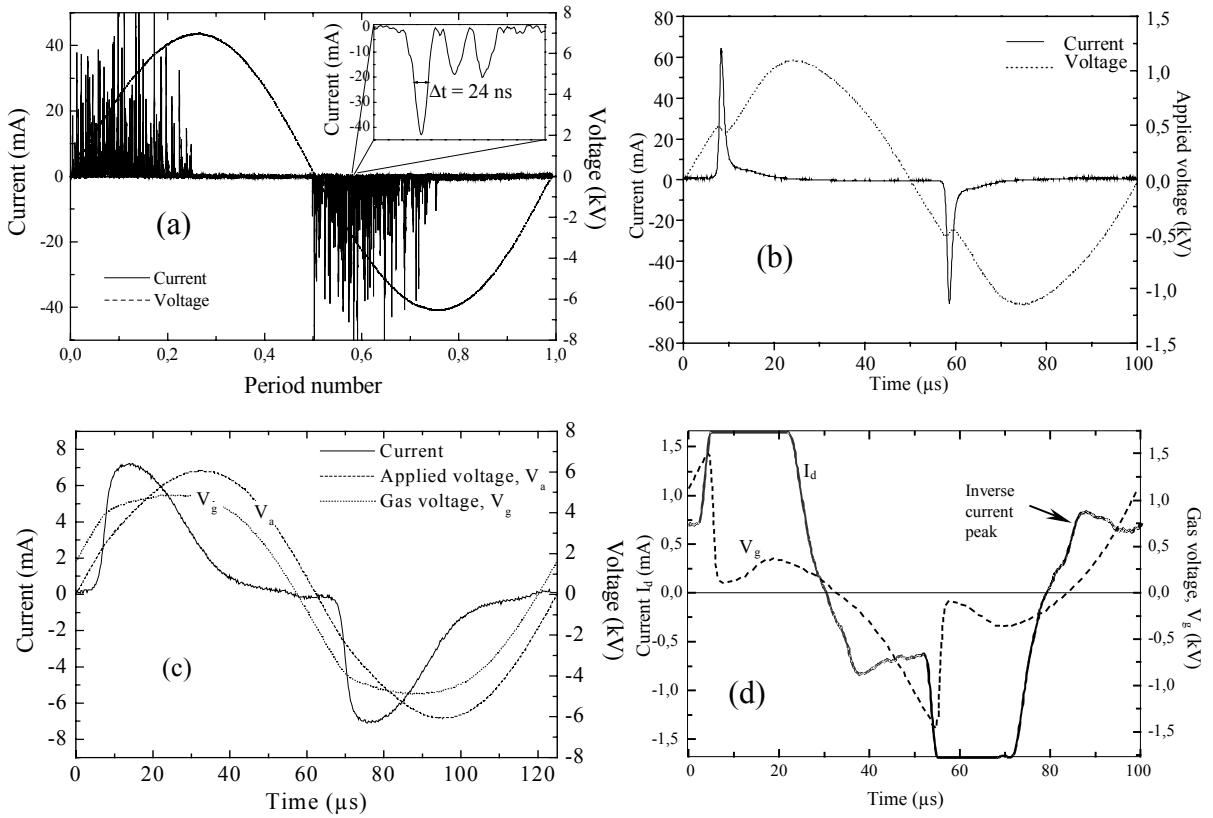

Figure 1 : Typical oscillogram of the power supply voltage and the discharge current of **a)** a filamentary DBD, **b)** a glow DBD in He**, c)** a glow DBD in N_2, V_g is the voltage applied to the gas. **d)** Zoom on a He DBD current and voltage applied to the gas

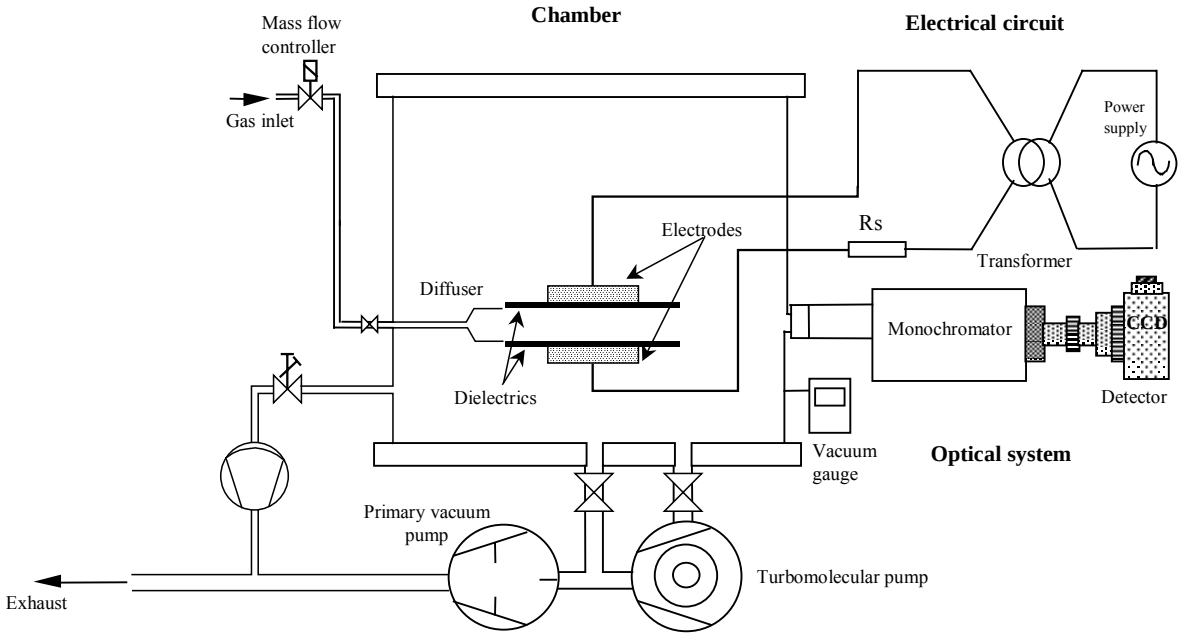

Figure 2 : Experimental set-up used for the different measurements.

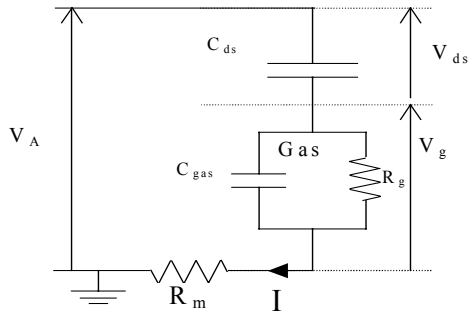

Figure 3: Electrical circuit equivalent of the discharge cell

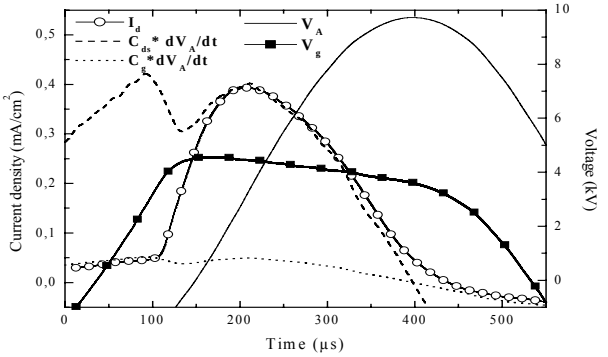

Figure 4: Comparison of thecurrent in N_2 glow DBD and $C_{ds}dV_A/dt$ and C_gdV_A/dt

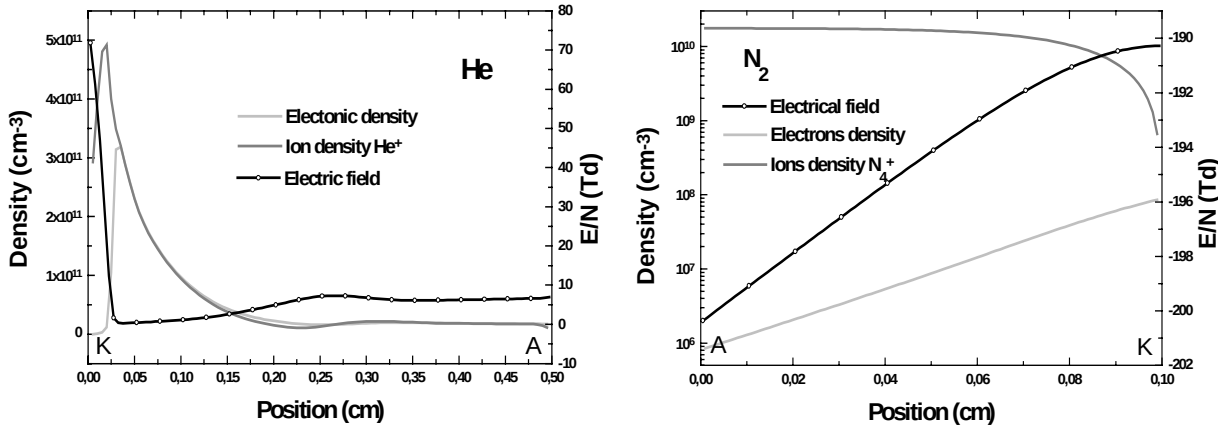

Figure 5: Space distribution of the electrical field and the ion and electron densities when the glow DBD maximum current is reached in He and in N_2.

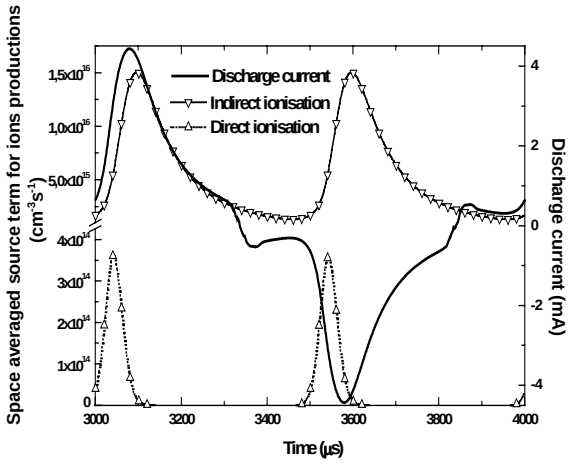

Figure 6: Time variations of the space integrated source terms characterising direct and indirect ion production

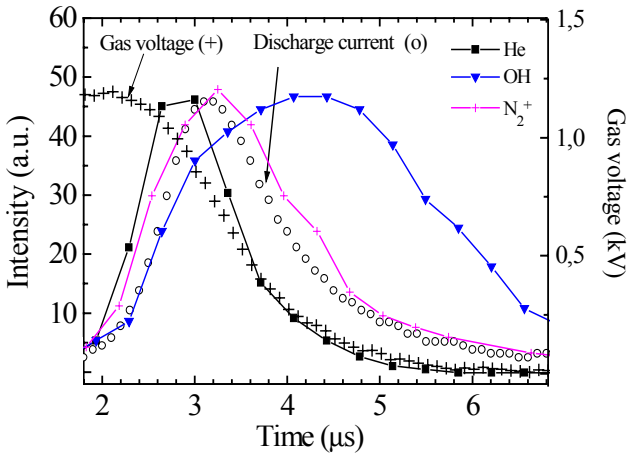

Figure 7: Time variations of He, N_2^+ and OH line and band intensities as well as those of the gas voltage, V_g, and the discharge current, I_d.

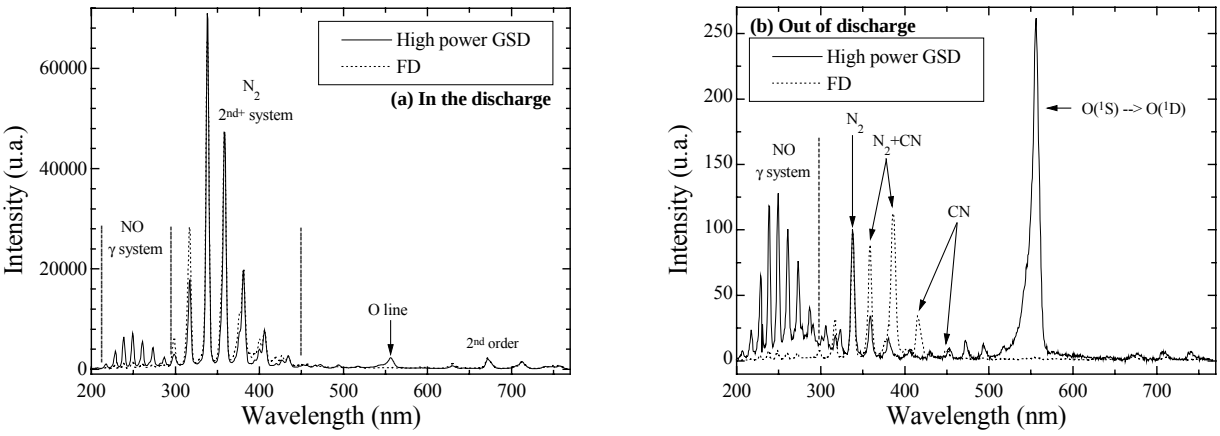

Figure 8: Emission spectra of glow DBD (1kHz) and filamentary DBD (4kHz) measured **a)** in the discharge and **b)** out of discharge

GDBD
FDBD

GDBD
FDBD

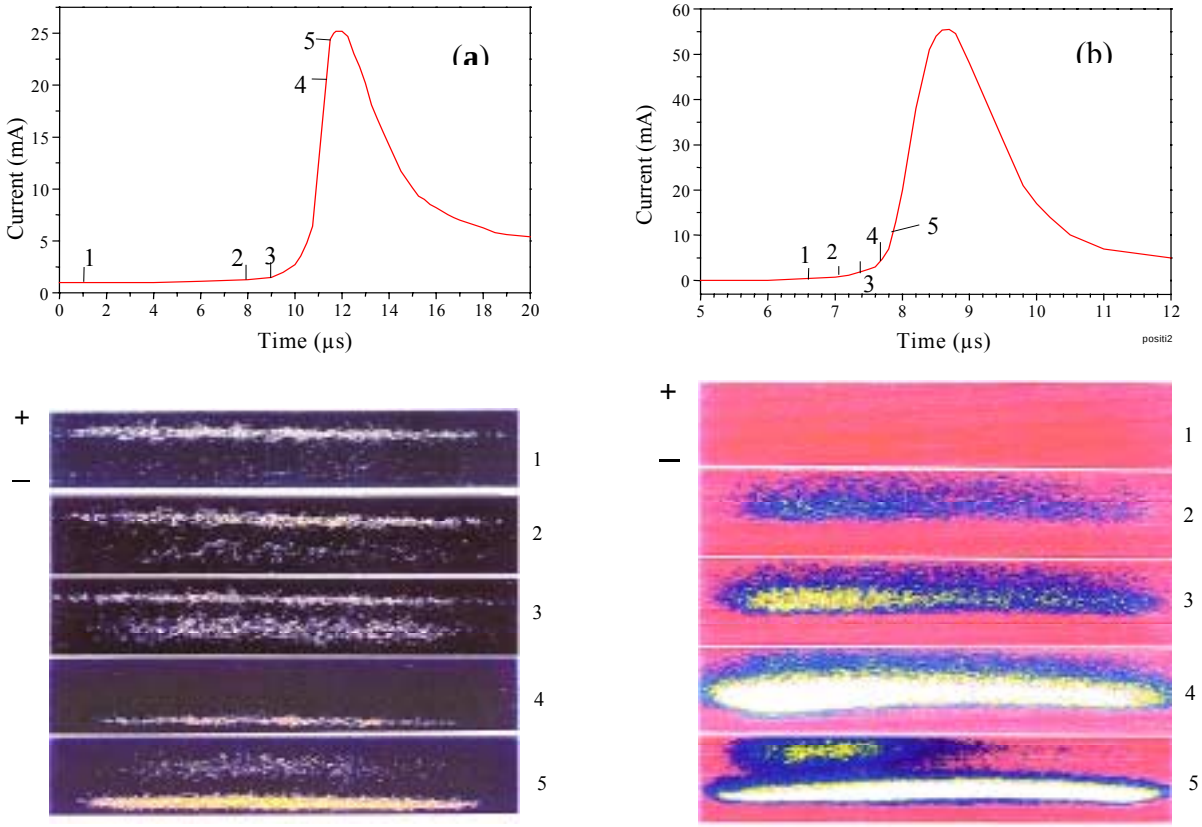

Figure 9: Short exposure time pictures of the gas gap and associated discharge current indicating the instant at which each picture was taken. **a)** Development of a glow DBD, the exposure time is100 ns for the pictures 1 to 3 and 10 ns for the pictures 4 and 5, **b)** development of a homogeneous DBD, the exposure time is 100 ns.

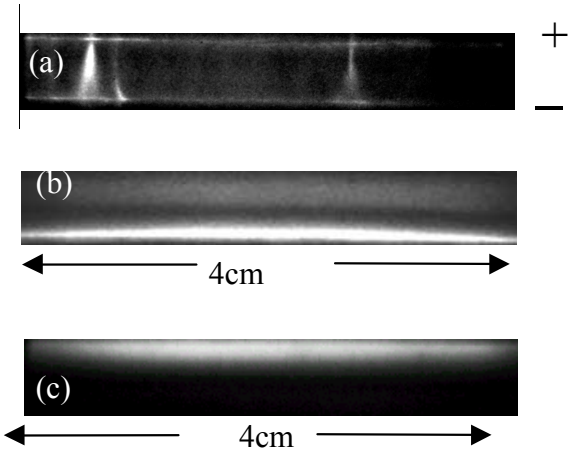

Figure 10: 10 ns exposure time picture of **a)** a filamentary DBD **b)** a glow DBD in He when the discharge current is maximum and **c)** a glow DBD in N_2 when the discharge current is maximum.

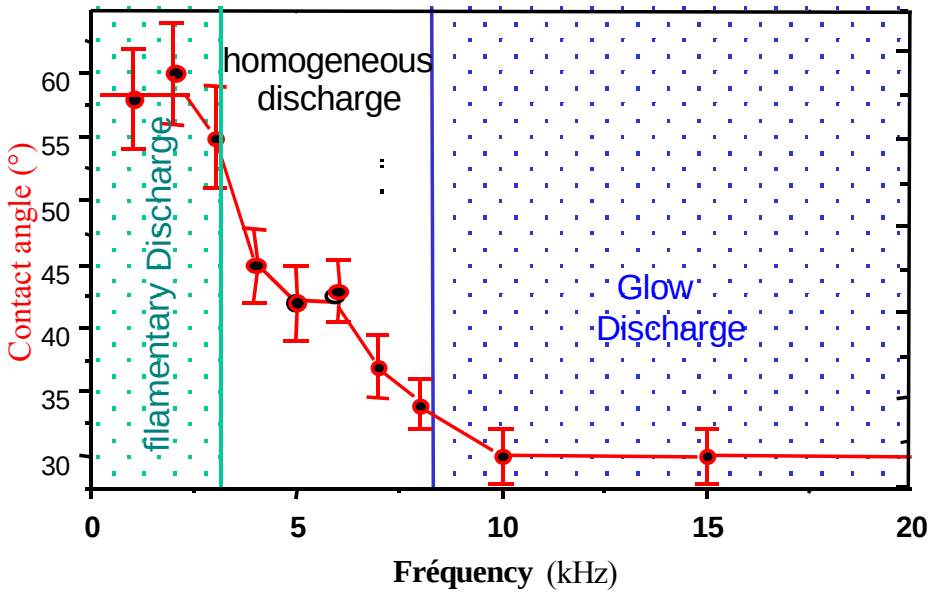

Figure 11 : Evolution of the contact angle of water drops deposited on the polypropylene as a function of the excitation frequency of a He DBD, all other parameters remaining constant.

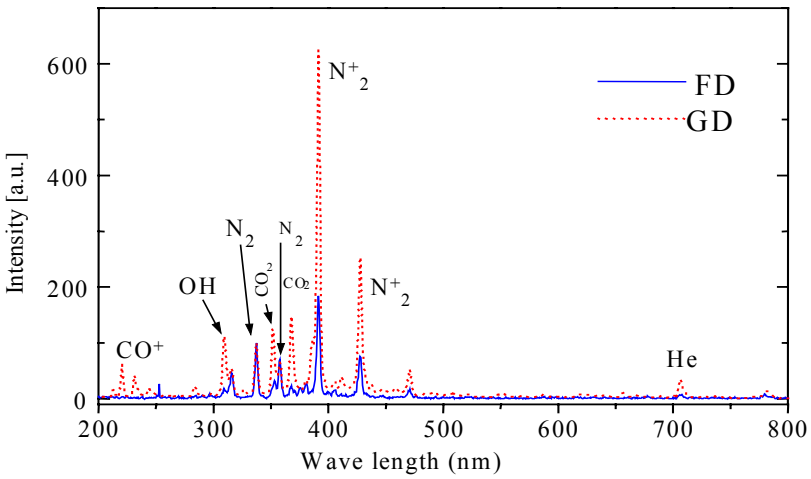

Figure 12 : Emission spectra of a filamentary DBD (line) and glow DBD (dot line) in He normalised on the N_2 emission at 337 nm